

Asymmetric Addition of Dimethylzinc to Benzaldehyde Catalyzed by (2*S*)-3-*exo*-(Dimethylamino)isobornenol. A Theoretical Study on the Origin of Enantioselection

Masashi Yamakawa[†] and Ryoji Noyori^{*,‡}

Kinjo Gakuin University, Omori, Moriyama, Nagoya 463-8521, Japan, and Department of Chemistry and Research Center for Materials Science, Nagoya University, Chikusa, Nagoya 464-8602, Japan

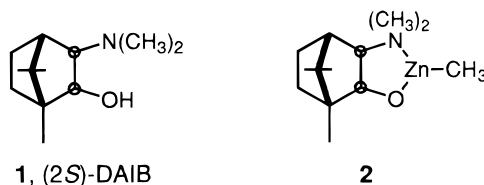
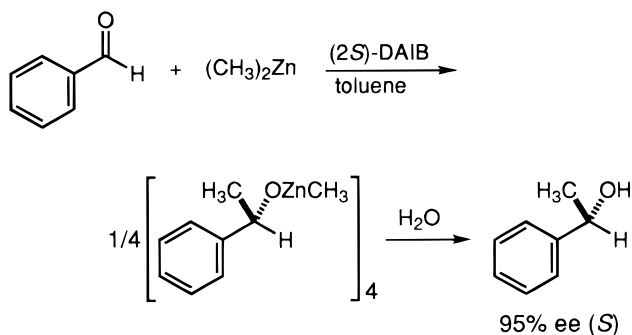
Received September 1, 1998

The asymmetric reaction of dimethylzinc and benzaldehyde in the presence of (2*S*)-3-*exo*-(dimethylamino)isobornenol ((2*S*)-DAIB) proceeds via a methylzinc aminoalkoxide/dimethylzinc/benzaldehyde mixed-ligand complex. Molecular orbital and density functional calculations revealed that the asymmetric bias is generated in the intramolecular methyl-transfer step by differences in the stabilities of the four diastereomeric transition structures. The anti-configured 5/4/4 tricyclic structures are favored over the syn tricyclic transition states that exhibit electrostatic repulsion between the 1,3-*syn*-oriented Zn–CH₃ groups. The steric origins of enantioselectivity are (1) the high stereodifferentiating ability of the bornane skeleton of DAIB and (2) nonbonded repulsion between the unreactive Zn–CH₃ spectator and the aldehyde phenyl group (anti structure) or between the DAIB *N*-CH₃ group and the migrating methyl group and/or carbonyl substituent (syn structure). The ground-state Zn complexes and transition states involved in this organometallic reaction are characterized by flexible frameworks arising from the electrostatic nature of the Zn–heteroatom interaction. The calculated transition states explain many experimental findings, including the substituent effects on the rate and enantioselectivity in methylation of *p*-substituted benzaldehydes.

Introduction

Asymmetric addition of diorganozincs to aldehydes catalyzed by chiral β -amino alcohols provides a general method for the preparation of chiral secondary alcohols.¹ We found that (2*S*)-3-*exo*-(dimethylamino)isobornenol ((2*S*)-DAIB; **1**) acts as a particularly efficient promoter for this asymmetric reaction.^{1–4} For example, as illustrated in Scheme 1, reaction of benzaldehyde and dimethylzinc (1:1 molar ratio) in toluene containing 0.02 mol of (2*S*)-DAIB at 25 to 40 °C gives, after aqueous workup, (*S*)-1-phenylethanol in up to 95% ee and in high yield.^{1–4} The presence of an electron-donating substituent at the para position of substrates tends to decrease the rate and enantioselectivity of methylation.³ Many lines of evidence indicate that the methylzinc ami-

Scheme 1. Asymmetric Addition of Dimethylzinc to Benzaldehyde Catalyzed by (2*S*)-3-*exo*-(Dimethylamino)isobornenol



noalkoxide **2** is the true catalyst and that the alkyl transfer reaction occurs according to Scheme 2.^{3–7} The initially formed mixed-ligand complex **3** undergoes

[†] Kinjo Gakuin University.

[‡] Nagoya University.

(1) Reviews: (a) Noyori, R.; Kitamura, M. *Angew. Chem., Int. Ed. Engl.* **1991**, *30*, 49–69. (b) Noyori, R. *Asymmetric Catalysis in Organic Synthesis*; Wiley: New York, 1994; Chapter 5. (c) Soai, K.; Niwa, S. *Chem. Rev.* **1992**, *92*, 833–856. The first example: Oguni, N.; Omi, T. *Tetrahedron Lett.* **1984**, *25*, 2823–2826.

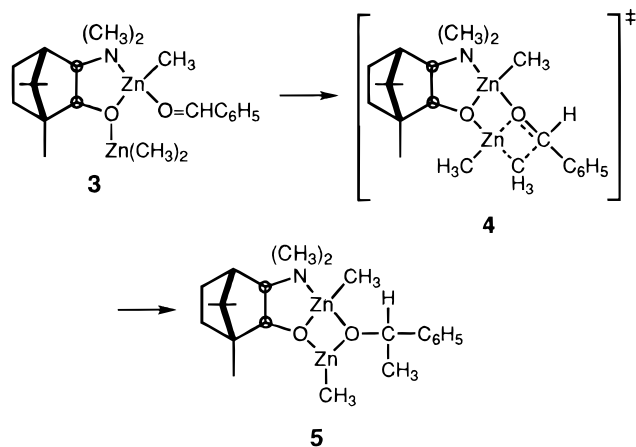
(2) (a) Kitamura, M.; Suga, S.; Kawai, K.; Noyori, R. *J. Am. Chem. Soc.* **1986**, *108*, 6071–6072. (b) Noyori, R.; Suga, S.; Kawai, K.; Okada, S.; Kitamura, M.; Oguni, N.; Hayashi, M.; Kaneko, T.; Matsuda, Y. *J. Organomet. Chem.* **1990**, *382*, 19–37. (c) Noyori, R.; Suga, S.; Kawai, K.; Okada, S.; Kitamura, M. *Pure Appl. Chem.* **1988**, *60*, 1597–1606.

(3) Kitamura, M.; Oka, H.; Noyori, R. *Tetrahedron*, in press. The Hammett plots of methylation of para-substituted benzaldehydes afforded a ρ value of +1.2. The ee values of alcohols derived from *p*-CF₃-, *p*-CH₃-, and *p*-CH₃OC₆H₄CHO were 96, 94, and 88%, respectively.

(4) Kitamura, M.; Suga, S.; Oka, M.; Noyori, R. *J. Am. Chem. Soc.* **1998**, *120*, 9800–9809.

(5) (a) Kitamura, M.; Yamakawa, M.; Oka, H.; Suga, S.; Noyori, R. *Chem. Eur. J.* **1996**, *2*, 1173–1181. (b) Kitamura, M.; Suga, S.; Niwa, M.; Noyori, R. Zhai, Z.-X.; Suga, H. *J. Phys. Chem.* **1994**, *98*, 12776–12781.

Scheme 2. Mechanism of the Alkyl Transfer Reaction



intramolecular methyl migration to give **5**, which is viewed as a catalyst/product complex. The product-forming complex **3** is regenerated from **5** upon reaction with dimethylzinc and benzaldehyde, where the formation of a stable methylzinc alkoxide dimer or tetramer (Scheme 1)^{6a,8} is essential for the operation of the catalytic cycle.⁷ The stereochemistry of the alkoxide product is kinetically determined at the transition state **4**. Here we elucidate the origin of enantiodifferentiation with the aid of *ab initio* molecular orbital (MO) and density functional calculations.⁹ Comparison of the structures of the diastereomers of **4**, combined with the simple model systems **6** consisting of 2-aminoethanol, dimethylzinc, and formaldehyde,⁷ provides an understanding of the mechanism of enantioselection. Although we intuitively selected (2*S*)-DAIB as an amino alcohol auxiliary, this study explains why it serves as an excellent chiral promoter.

Computational Procedure

All the calculations were performed using the GAUSSIAN 94 program.¹⁰ All geometries of transition states as well as ground-state molecules were optimized at the restricted Hartree-Fock level using the 3-21G basis set for H, C, N, and O and an all-electron [8s5p3d]/(14s9p5d) basis function¹¹ for Zn (RHF/3-21G/Zn). The frequency analysis was performed on the basis of the RHF calculations. The single-point energy was determined at the hybrid density functional B3LYP level by replacing the 3-21G basis functions for H, C, N, and O with

(6) (a) Kitamura, M.; Okada, S.; Suga, S.; Noyori, R. *J. Am. Chem. Soc.* **1989**, *111*, 4028–4036. (b) Kitamura, M.; Suga, S.; Niwa, M.; Noyori, R. *J. Am. Chem. Soc.* **1995**, *117*, 4832–4842.

(7) Yamakawa, M.; Noyori, R. *J. Am. Chem. Soc.* **1995**, *117*, 6327–6335.

(8) Boersma, J. In *Comprehensive Organometallic Chemistry*; Wilkinson, G., Ed.; Pergamon Press: New York, 1982; Chapter 16.

(9) A related system was examined by a semiempirical AM1 procedure using the fixed core coordinate obtained by an *ab initio* method:⁷ Vidal-Ferran, A.; Moyano, A.; Pericás, M. A.; Riera, A. *Tetrahedron Lett.* **1997**, *38*, 8773–8776.

(10) Frisch, M. J.; Trucks, G. W.; Schlegel, H. B.; Gill, P. M. W.; Johnson, B. G.; Robb, M. A.; Cheeseman, J. R.; Keith, T.; Petersson, G. A.; Montgomery, J. A.; Raghavachari, K.; Al-Laham, M. A.; Zakrzewski, V. G.; Ortiz, J. V.; Foresman, J. B.; Cioslowski, J.; Stefanov, B. B.; Nanayakkara, A.; Challacombe, M.; Peng, C. Y.; Ayala, P. Y.; Chen, W.; Wong, M. W.; Andres, J. L.; Replogle, E. S.; Gomperts, R.; Martin, R. L.; Fox, D. J.; Binkley, J. S.; Defrees, D. J.; Baker, J.; Stewart, J. P.; Head-Gordon, M.; Gonzalez, C.; Pople, J. A. *Gaussian 94*, Revision D.4; Gaussian, Inc., Pittsburgh, PA, 1995.

(11) Poirier, R.; Kari, R.; Ciszmadia, I. G. *Handbook of Gaussian Basis Sets*; Elsevier: Amsterdam, 1985.

Table 1. Calculated Energies of 3–5

structure	3-21G/Zn//3-21G/Zn, ^a hartree (kcal/mol) ^b	imag freq, ^c cm ⁻¹	ZPC, ^c kcal/ mol	B3LYP/6-31G*/Zn// 3-21G/Zn, ^a hartree (kcal/mol) ^d
<i>anti</i> - 3	-4608.2871 (0.0)		369.4	-4624.3886 (0.0)
<i>syn</i> - 3	-4608.2861 (0.7)		370.3	-4624.3875 (1.6)
<i>lin</i> - 3	-4608.2846 (1.6)		369.5	-4624.3860 (1.7)
<i>anti</i> - <i>Si</i> - 4	-4608.2541 (20.7)	437i	369.8	-4624.3587 (19.2)
<i>anti</i> - <i>Re</i> - 4	-4608.2492 (23.8)	437i	370.2	-4624.3537 (22.7)
<i>syn</i> - <i>Re</i> - 4	-4608.2499 (23.3)	413i	369.7	-4624.3527 (22.9)
<i>syn</i> - <i>Si</i> - 4	-4608.2470 (25.2)	424i	369.8	-4624.3515 (23.7)
(<i>S</i>)- 5	-4608.3533 (-41.6)		373.1	-4624.4362 (-26.2)
(<i>R</i>)- 5	-4608.3518 (-40.5)		373.0	-4624.4344 (-25.2)

^a For Zn, an all-electron basis set was used. ^b Relative energies. ^c Unscaled zero-point correction. ^d Relative energies with ZPC.

6-31G(d) (B3LYP/6-31G*/Zn//3-21G/Zn). The natural bond orbital population analysis (NPA/NBO)¹² was carried out at the B3LYP/6-31G*/Zn level. The results are summarized in Table 1. The calculated structures of **3–6** are shown in Figures 1 and 2.

Results and Discussion

Catalyst **2** possessing a Zn^{δ+}–O^{δ-} dipole acts as a bifunctional catalyst.⁷ The Lewis acidic Zn atom accommodates the oxygen atom of benzaldehyde, whereas the adjacent basic O atom accepts dimethylzinc at Zn. The bornane skeleton provides a clear distinction between the “exo” and “endo” diastereofaces in the aminoalkoxide catalyst **2**. The presence of the geminal methyl groups leads to the endo-selective coordination of the aldehyde with the Zn center. The donor/acceptor complexation leads to the reactive mixed-ligand complexes **3** with various conformations.¹³ The MO calculation suggests that the *anti*-**3** structure^{7,14} is the most stable form, in which the C=O linkage is arranged anti to the five-membered Zn aminoalkoxide ring via the Zn(1)–O(10) bond (Figure 1). The aldehyde to Zn(1) dative bond is rather weak,¹⁵ as judged from the near-trigonal-pyramidal geometry of Zn(1) with a sum of the three bond angles of 352.8°. The benzaldehyde ligand is planar in order to achieve the full conjugation of the C=O moiety with the phenyl group, and the molecular plane bisects the N(5)–Zn(1)–O(2) angle. By this complexation, the aldehyde is electrophilically activated, as suggested by the longer C=O bond of 1.225 Å, compared with 1.211 Å in free benzaldehyde. The tricoordinate Zn(7) atom has a flat geometry. Upon interaction of dimethylzinc with O(2), both C(8)H₃ and C(9)H₃ on Zn(7) become significantly nucleophilic, as suggested by

(12) (a) Glendenig, E. D.; Reed, A. E.; Carpenter, J. E.; Weinhold, F. NBO, version 3.1; Gaussian, Inc., Pittsburgh, PA, 1995. (b) Reed, A. E.; Weinstock, R. B.; Weinhold, F. *J. Chem. Phys.* **1985**, *83*, 735–746. (c) Reed, A. E.; Curtiss, L. A.; Weinhold, F. *Chem. Rev.* **1988**, *88*, 899–926.

(13) Review on the structures of Lewis acid-carbonyl compound complexes: Shambayati, S.; Crowe, W. E.; Schreiber, S. L. *Angew. Chem., Int. Ed. Engl.* **1990**, *29*, 256–272.

(14) (a) Evans, D. A. *Science* **1988**, *240*, 420–426. (b) Corey, E. J.; Yuen, P.-W.; Hannon, F. J.; Wierda, D. A. *J. Org. Chem.* **1990**, *55*, 784–786.

(15) (a) Haaland, A. *Angew. Chem., Int. Ed. Engl.* **1989**, *28*, 992–1007. (b) Jonas, V.; Frenking, G.; Reetz, M. T. *J. Am. Chem. Soc.* **1994**, *116*, 8741–8753.

(16) (a) Corey, E. J.; Rohde, J. J.; Fischer, A.; Azimiora, M. D. *Tetrahedron Lett.* **1997**, *38*, 33–36. (b) Corey, E. J.; Rohde, J. J. *Tetrahedron Lett.* **1997**, *38*, 37–40. (c) Corey, E. J.; Barnes-Seeman, D.; Lee, T. W. *Tetrahedron Lett.* **1997**, *38*, 1699–1702. (d) Corey, E. J.; Barnes-Seeman, D.; Lee, T. W. *Tetrahedron Lett.* **1997**, *38*, 4351–4354. (e) Corey, E. J.; Barnes-Seeman, D.; Lee, T. W.; Goodman, S. N. *Tetrahedron Lett.* **1997**, *38*, 6513–6516.

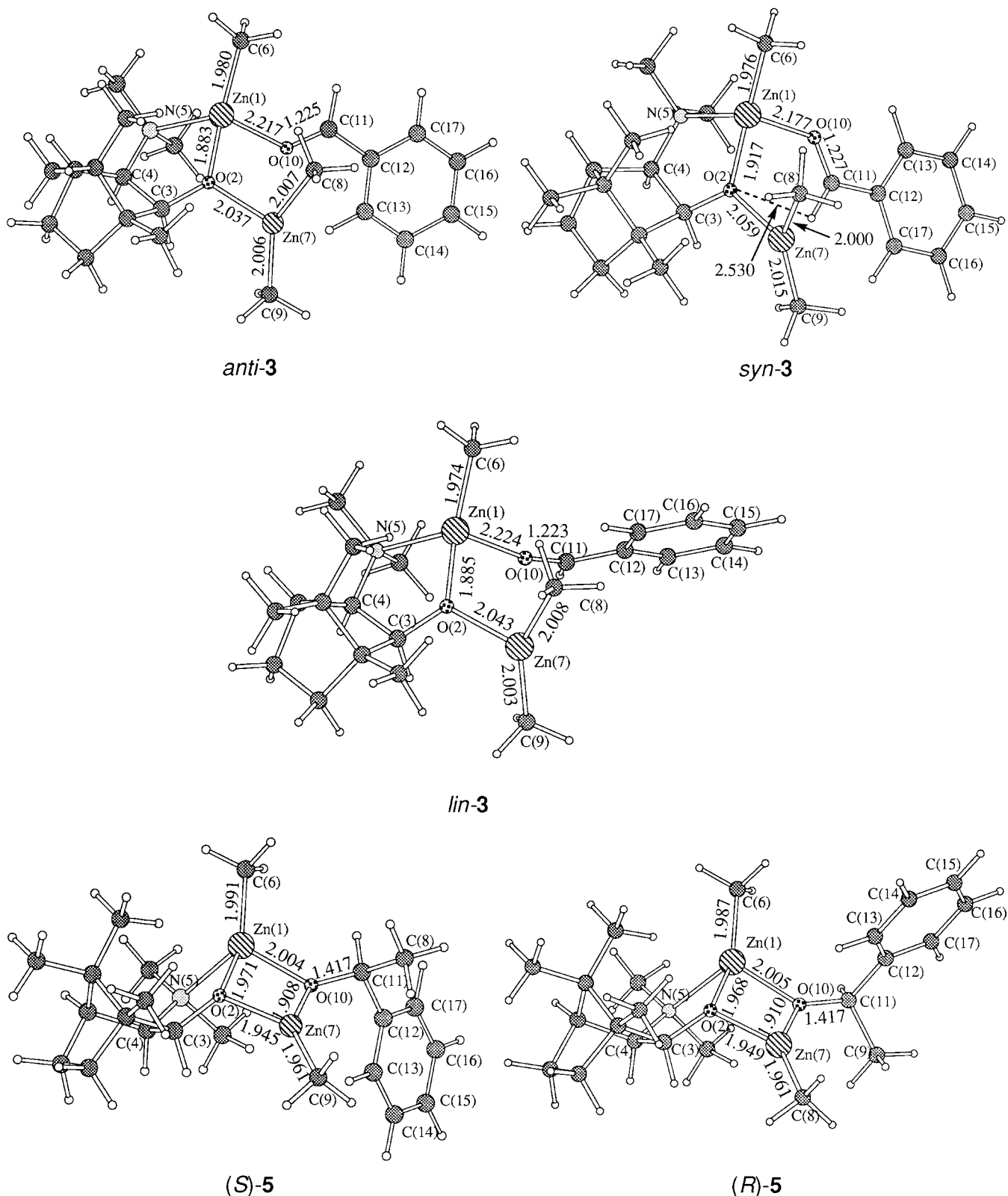


Figure 1. Structures of **3** and **5** optimized at the RHF/3-21G/Zn level.

the 2.7% increase in the length of the Zn(7)–CH₃ bonds from that of the free state (2.007 vs 1.955 Å). In contrast, the Zn(1)–CH₃ distance is rather short at 1.980 Å and this methyl group remains an unreactive spectator during the reaction. The calculation also predicts the presence of *syn-3*, which has a syn arrangement with respect to the amino alkoxide ring and O(10)–C(11) bond. The Zn(1)–O(10)/C(11)–C(12) relation is anti, as

is seen in *anti-3*. This structure is stabilized by a Coulombic interaction (2.530 Å) between the formyl hydrogen (+0.18 au) and the O(2) atom (−0.61 au),^{7,16} while other parameters are similar to those of *anti-3*. Non-hydrogen-bonded syn isomers are not present as energy minima. In addition, the third structure, *lin-3*, was detected, which has a near-linear Zn(1)–O(10)–C(11) arrangement (167.6°).¹⁷ The complexes *syn-3* and

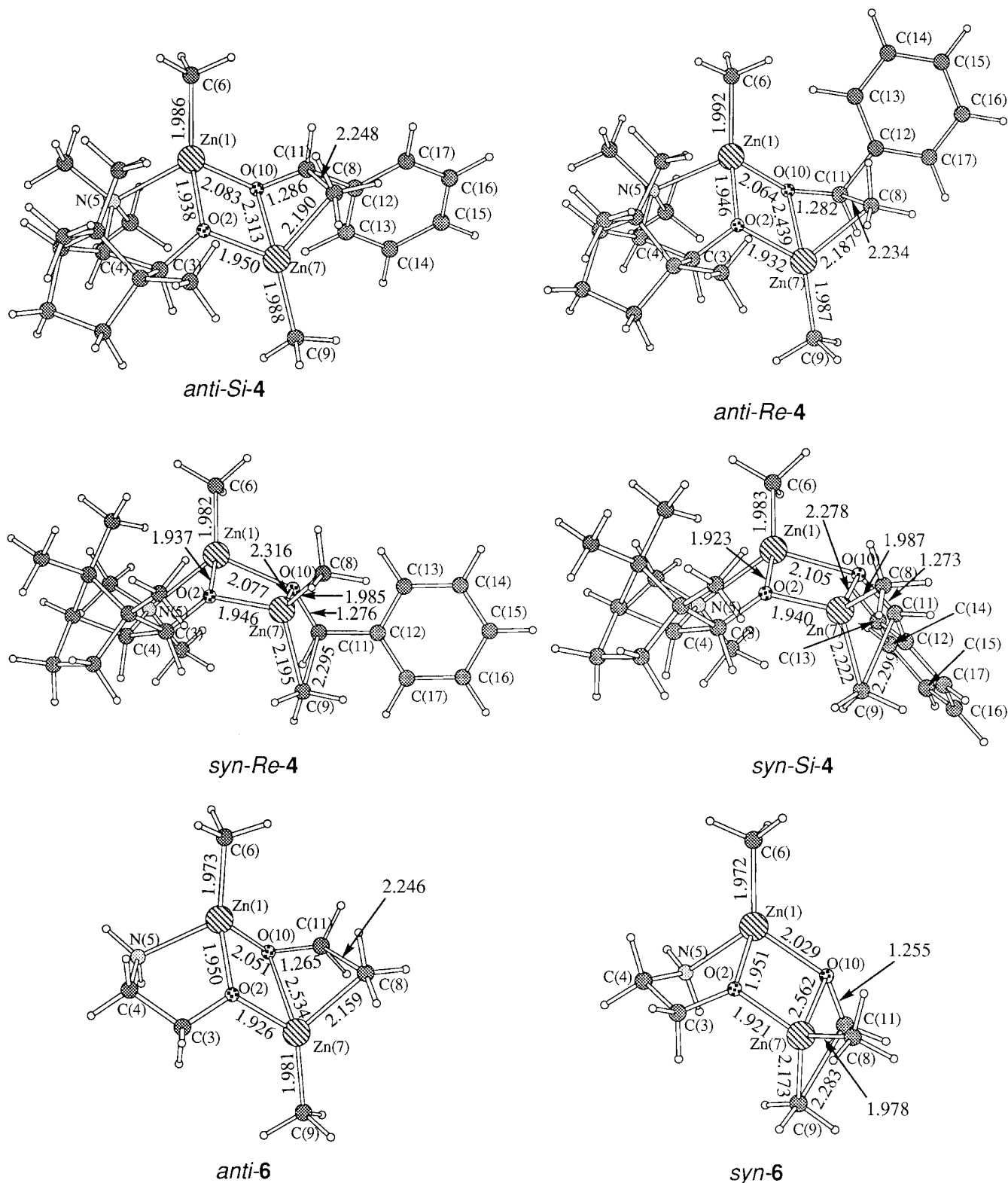


Figure 2. Structures of transition states **4** and **6** optimized at the RHF/3-21G/Zn level.

lin-3 are less stable than *anti-3* by only 1.6 and 1.7 kcal/mol at the B3LYP/6-31G*/Zn level, respectively.

Complex **3** causes methyl migration from Zn(7) to the aldehyde carbon by way of transition state **4**, resulting in either (*S*)- or (*R*)-**5**. Product **5**, having a planar Zn₂O₂ four-membered ring (Figure 1), is very stable, and this reaction takes place with an exothermicity as high as 26 kcal/mol at the B3LYP level. The diastereomeric

products, (*S*)- and (*R*)-**5**, have very similar energy and structural parameters.

The complexes **3** are geometrically flexible because of the electrostatic nature of the O(10) to Zn(1) dative bond.^{7,15} The energy barriers for rotation about the Zn(1)–O(10) and O(2)–Zn(1) bonds are also low. Therefore, **3** undergoes alkyl-transfer reactions via various transition states utilizing the endo face. The transition

structures **4** are characterized by the 5/4/4 tricyclic geometries fused with the bornane skeleton, and the MO calculation suggests the presence of anti and syn configurations with respect to the tricyclic structure.^{7,18} These geometries, coupled with the prochirality of benzaldehyde possessing *Si* and *Re* faces, make four diastereomeric transition states possible, as illustrated in Figure 2. The absolute configuration of the final product is determined by the relative stabilities of the diastereomeric structures. The *S* product, (*S*)-**5**, is derived via *anti-Si-4* and *syn-Si-4*, while the *R* stereoisomer is obtained via *anti-Re-4* and *syn-Re-4*. The calculations indicate that the stability decreases in the order *anti-Si-4* > *anti-Re-4* ≈ *syn-Re-4* > *syn-Si-4*. Each structure possesses a single imaginary frequency. The energies of these transition structures are higher than **3** by 19.2, 22.7, 22.9, and 23.7 kcal/mol at the B3LYP level, respectively (Table 1). The most favored *S*-generating structure, *anti-Si-4*, is 3.5 kcal/mol more stable than the *R*-forming structure *anti-Re-4* that is close to *syn-Re-4*. Geometrically, *anti-Si-4* is closely correlated with *anti-3*, in which the *Si* face of benzaldehyde is exposed to the dimethylzinc moiety, whereas the structure of *syn-Re-4* resembles that of *syn-3*, where the *Re* aldehyde face is accessible. The linear complex, *lin-3*, likely undergoes methyl migration via *anti-Re-4* or *syn-Re-4*.

Both electronic and steric factors are important for the stability of the transition states. Since steric repulsions between substituents are absent in the model systems **6** (Figure 2),¹⁹ the lower stability of *syn-6* compared to *anti-6* ($\Delta E = 2.9$ kcal/mol) is due basically to electronic effects, as discussed for related ground-state molecules.^{5a,7} The closest C(3)H...HC(9) distance in *syn-6* is 2.659 Å, which is much longer than the 2.4 Å distance of the van der Waals contact. The calculated NPA charges at the C(6)H₃ and C(8)H₃ groups are -0.67 and -0.65 au, respectively. Thus, the primary factor that destabilizes this structure is the electrostatic repulsion of the 1,3-syn-oriented, nonreacting Zn-CH₃ groups in the central four-membered ring. Such an undesired effect is absent in *anti-6*.

All the transition structures of methyl migration, **4**, are stabilized by the pericyclic cooperation of the six atoms, Zn(1), O(2), Zn(7), C(8), C(11), and O(10).⁷ The most stable transition state, *anti-Si-4*, is spatially very close to *anti-3*, leading to the major reaction pathway. Thus, *anti-3*, upon slight downward bending of the O(2)-Zn(7) linkage, readily delivers the C(8)H₃ group to the C(11) center. When the *anti-3* and *anti-Si-4* structures are compared, the bond shortening and lengthening occur alternately; O(10)-Zn(1) and O(2)-Zn(7) are shortened, but Zn(1)-O(2), Zn(7)-C(8), and C(11)=O(10) are lengthened. In *anti-Si-4*, the Zn(7)-

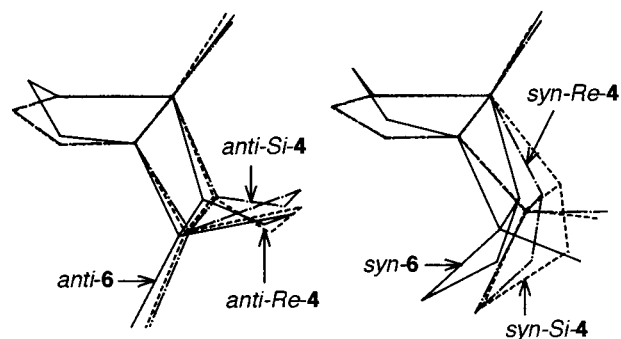


Figure 3. Comparison of the 5/4/4 core geometries of **4** and **6**.

C(8) bond length is increased by 9% from *anti-3* becoming 2.190 Å, and the bond-forming C(8)-C(11) distance becomes 2.248 Å. This transition state (and also other diastereomers) contains a reacting benzaldehyde with a planar geometry, thereby neutralizing a positive charge developed at C(11) in the methyl-transfer step. Thus, this most favored transition structure possesses an electronically favored anti-5/4/4 tricyclic alignment which contains little steric constraint, suitably accommodating the substituents in space. The activation energy of the reaction via *anti-Si-4* is 6.0 kcal/mol larger than the value of the model reaction via *anti-6* at the B3LYP level. As shown in Figure 3, the core framework of *anti-Si-4* is similar to that of the model *anti-6*,⁷ the only major differences being the larger N(5)-Zn(1)-O(10) angle (111.0 and 102.3°) and the smaller Zn(1)-O(10)-C(11) angle (118.5 vs 122.9°).¹⁹

In general, molecular structures tend to be stabilized through maximizing electron delocalization while minimizing steric constraints. In both anti and syn tricyclic structures, nonbonded repulsions of substituents are mitigated by appropriate modifications of bond lengths and angles in different ways, depending on the respective structure. Most notably, the Zn(1)-N(5), Zn(1)-O(10), Zn(7)-C(8) (or Zn(7)-C(9)), and Zn(7)-O(10) interactions in **4** are highly electrostatic in nature,⁷ making the atomic arrangements highly flexible. The core structures of the second to fourth transition states are thus largely distorted from the model geometries **6**, as compared schematically in Figure 3.^{19,20} The second stable transition structure *anti-Re-4* is 3.5 kcal/mol above *anti-Si-4*. The destabilization of this structure appears to arise mainly from nonbonded repulsion between the nonreacting methyl group at Zn(1) and the bulky phenyl group of the aldehyde, as judged from the C(6)H₃...HC(13) distance of 2.383 Å, which is shorter than the sum of the van der Waals radii of 2.4 Å. To mitigate this undesired effect, in going from *anti-Si-4* to *anti-Re-4*, the Zn(1)-O(10)-C(11) angle is increased from 118.5° to 138.0°, which can also be compared with the angle of 122.9° in the model *anti-6*.⁷

The syn tricyclic transition structures are less stable than the anti structures for the electronic reason described above. The NPA charges of the C(6)H₃ and C(8)H₃ groups in both *syn-Re-4* and *syn-Si-4* are -0.67 and -0.65 to -0.66 au, respectively. In *syn-4*, the Zn-CH₃/C₆H₅ nonbonded repulsion is absent but now the

(17) (a) Loncharich, R. J.; Schwartz, T. R.; Houk, K. N. *J. Am. Chem. Soc.* **1987**, *109*, 14-23. (b) Nelson, D. J. *J. Org. Chem.* **1986**, *51*, 3185-3186. (c) Raber, D. J.; Janks, C. M.; Johnston, M. D., Jr.; Raber, N. K. *J. Am. Chem. Soc.* **1980**, *102*, 6591-6594. (d) Fukuzumi, S.; Okamoto, T.; Fujita, M.; Otera, J. *J. Chem. Soc., Chem. Commun.* **1996**, 393-394.

(18) The calculation of the model system suggested the possibility of an additional chairlike six-membered transition state which is considerably less stable than *anti*- and *syn-6*.

(19) The model **6**, lacking the bornane skeleton, is structurally more relaxed than the real system **4**. The five-membered ring is skewed by rotation about the C(3)-C(4) bond, while the N(5)-C(4) and O(2)-C(3) linkages in **4** are eclipsed.

(20) The application of the model core coordinates to the real system⁹ is not appropriate for correct prediction.

endo-oriented $N\text{-CH}_3$ group in the DAIB skeleton interacts with carbonyl substituents. This repulsive effect is observed even with *syn-Re-4*. In fact, the $\text{N}(5)\text{-CH}_3\cdots\text{HC}(11)$ distance of 2.289 Å is much less than the 2.4 Å for the van der Waals contact, suggesting a repulsive interaction between these hydrogens. The $\text{N}(5)\text{-Zn}(1)\text{-O}(10)$ angle, 117.1°, in *syn-Re-4* is significantly larger than the 103.9° in simple *syn-6*.⁷ The $\text{C}(3)\text{H}\cdots\text{HC}(9)$ distance is 2.468 Å. This structure is less stable than *anti-Si-4* by 3.7 kcal/mol. The steric congestion is even more conspicuous in *syn-Si-4*, the least stable transition structure (0.8 kcal/mol above *syn-Re-4*). The serious $N\text{-CH}_3/\text{C}_6\text{H}_5$ repulsion is actually minimized at the cost of significant distortion of the core tricyclic framework. Now the $\text{N}(5)\text{-Zn}(1)\text{-O}(10)$ angle becomes 128.2°, while the endo $\text{N}(5)\text{CH}_3\cdots\text{C}(13)$ distance of 3.027 Å is very close to 2.9 Å, the sum of the van der Waals radii of hydrogen and carbon. Furthermore, the $\text{N}(5)\text{CH}_3\cdots\text{HC}(9)$ distance of 2.360 Å is much shorter than the 2.872 Å in *syn-Re-4*. Thus, this *syn* structure is destabilized by an additional $N\text{-CH}_3/\text{Zn-CH}_3$ repulsion.⁹

A number of earlier experimental observations can be understood by this theoretical study. For example, the calculated transition structures agree with (1) the sense of asymmetric induction observed in the actual catalysis (Scheme 1),² (2) the lack of reactivity of ketonic substrates,^{2,21} (3) the increased enantioselectivity with the larger diethylzinc compared with dimethylzinc,² and (4) the notable effects of the steric bulk of nitrogen substituents on enantioselectivity in related reactions.²²

It should be noted that, in both starting complexes **3** and transition states, even in the sterically congested *syn-4*, the benzaldehyde has a planar geometry securing a full $\text{C}=\text{O}/\text{C}_6\text{H}_5$ conjugation. This electronic effect, inducing conformational rigidity, is reflected in the high enantioselectivity of the alkylation of aromatic aldehydes.²

Furthermore, this calculation sheds light on the unique substituent effects observed experimentally.³ Because of the difference in the charge distributions of **3** and **4**, the electronic properties of para substituents in benzaldehydes significantly affect the activation energy. The NPA charge at C(11) of +0.30 au in the transition state *anti-Si-4* is smaller than +0.63 au in the starting complex *anti-3*. Thus, electron-donating substituents would increase the activation energy and, consequently, reduce the reaction rate.³ The single-point energy calculations on the optimized *anti-3* and *anti-Si-4* structures with an added para substituent are consistent with this expectation. Introduction of a CH_3O or CH_3 group to the para position of benzaldehyde increases the activation energy by 1.6 and 0.6 kcal/mol at the B3LYP level, respectively, while placement of a $p\text{-CF}_3$ group lowers the value by 2.0 kcal/mol. The

energies of *anti-Re-4* and *syn-Re-4* are very close, and the relative stabilities of these second and third transition structures are subtly influenced by further electronic and steric perturbations. The notable substituent effects on the degree of enantioselectivity³ are understood in terms of the difference in the electronic structures of the anti and *syn* transition structures, although the accuracy of the present calculation does not allow for a quantitative treatment. The *syn* structures are characterized by a high positive charge at C(11) compared to the anti structures. Since the NPA charge of +0.32 au in *syn-Re-4* is definitely (7%) larger than the +0.30 au in *anti-Si-4* or *anti-Re-4*, an electron-releasing group such as $p\text{-CH}_3\text{O}$ stabilizes the *syn* structure more. Thus, enhanced contribution of the *R*-generating *syn-Re-4*-type transition state results in a decrease of the ee value of the *S* alcoholic product. The $p\text{-CF}_3$ group exerts an opposite influence.³

Conclusion

This theoretical study predicts that the (2*S*)-DAIB-promoted asymmetric methylation of benzaldehyde giving *S*-enriched 1-phenylethanol occurs from the mixed-ligand complexes **3** mainly via anti-configured 5/4/4 tricyclic transition states. The *syn* tricyclic structures are less favored because of the electrostatic repulsion between the two nonreacting Zn-CH_3 groups in the central four-membered ring. The steric origins of enantioselectivity are, in addition to the high stereodifferentiating ability of the bornane skeleton of (2*S*)-DAIB,⁵ the nonbonded repulsions between the unreactive Zn-CH_3 spectator and the phenyl substituent in the aldehyde (in *anti-4*) or between the $N\text{-CH}_3$ group in the chiral auxiliary and the migrating methyl group and/or carbonyl substituent (in *syn-4*). Thus, the complex *anti-3* undergoes intramolecular methyl transfer mostly through *anti-Si-4* via slight geometrical changes to form (*S*)-**5**. This transition structure possesses an electronically favored anti 5/4/4 tricyclic alignment, avoids steric repulsion of the bornane skeleton with the aldehyde and dimethylzinc, and minimizes nonbonded repulsion between the Zn-CH_3 group and carbonyl substituents. Diastereomeric *anti-Re-4* and *syn-Re-4* are less stable than *anti-Si-4* largely for a steric and an electronic reason, respectively. The structure *syn-Si-4* is disfavored on both electronic and steric grounds and is the least stable of the four diastereomers. These calculated transition structures reasonably explain a number of experimental findings.

Acknowledgment. This work was financially supported by a Grant-in-Aid for Scientific Research (No. 07CE2004) from the Ministry of Education, Science, Sports and Culture of Japan.

Supporting Information Available: Tables giving optimized structural data for **3-5**, including bond distances and bond angles (22 pages). Ordering information is given on any current masthead page.

OM9807405

(21) Dosa, P. I.; Fu, G. C. *J. Am. Chem. Soc.* **1998**, *120*, 445–446.

(22) Oguni, N.; Matsuda, Y.; Kaneko, T. *J. Am. Chem. Soc.* **1988**, *110*, 7877–7878.